Dose enhancement close to platinum implants for the 4, 6, and 10 MV stereotactic radiosurgery

Joel Y. C. Cheung
Brain Centre, Canossa Hospital, 1 Old Peak Road, Hong Kong

Ben K. P. Ng
Medical Physics Unit, Department of Clinical Oncology, Queen Mary Hospital, Hong Kong

K. N. Yu[a)]
Department of Physics and Materials Science, City University of Hong Kong, Tat Chee Avenue, Kowloon Tong, Hong Kong

(Received 28 April 2004; revised 12 July 2004; accepted for publication 3 August 2004; published 15 September 2004)

Three photon interaction processes, namely, the photoelectric effect, Compton effect, and pair production, can occur when materials with high atomic numbers are irradiated by the high- and low-energy bremsstrahlung photons from a linear accelerator. A dose enhancement, due to the photoelectric effect and pair production, near targets with platinum implants (with a high atomic number) in radiosurgery cannot be predicted by the XKnife® radiosurgery treatment planning system. In the present work, Monte Carlo simulations using PRESTA EGS4 were employed to investigate the resulting dose enhancements from 4, 6, and 10 MV energies commonly used in the stereotactic radiosurgery system. Dose enhancements from 32% to 68% were observed close to the platinum implant for the above energies when using a 12.5 mm collimator. Comparatively higher dose enhancements were observed when using smaller collimators. It was found that this dose enhancement increased with beam energy but decreased as beam size increased. © *2004 American Association of Physicists in Medicine.* [DOI: 10.1118/1.1797531]

Key words: XKnife®, Leksell Gamma Knife®, stereotactic radiosurgery, EGS4 Monte Carlo, platinum implant

INTRODUCTION

Platinum objects are sometimes implanted into a human brain, such as the Guglielme detachable coil (GDC) system,[1] the auditory brainstem implant (ABI),[2] etc. The GDC is used to obliterate the brain aneurysm and is suitable for patients who cannot have general aneurysm clipping. Soft platinum coils are deployed into the aneurysm under x-ray fluoroscopy. The ABI is designed to provide sound information to individuals with neurofibromatosis type 2, who will become deaf after the removal of bilateral tumors from the auditory nerves. The ABI has a specially designed platinum electrode. This electrode is placed on the surface of the cochlear nucleus in the brainstem, bypassing the inner ear and auditory nerve.

For patients who undergo radiosurgery and who have platinum implants inside their heads within the treatment arc, no specific guidelines or recommendations to minimize the undesired effects to the surrounding critical structures have been given.

The linear accelerator produces photons by the bremsstrahlung process to generate a spectrum of photon output. Photoelectric effect and pair production will occur when materials with high atomic numbers (e.g., platinum with $Z=78$) are irradiated with low-energy (energy <0.5 MeV) and high-energy (energy >4 MeV) photons, respectively.[3]

The XKnife® radiosurgery treatment planning system (TPS) is used for stereotactic radiosurgery of patients.[4] The dose calculations used a pencil beam algorithm that involved the maximum tissue ratio, off-axis ratio and the source-to-isocenter distance for different collimators. These parameters were measured in a water tank and the dose computation to a point was based on a homogeneous water medium, without taking the heterogeneity factor, if existed, into consideration. For any high-atomic-number implants inside the brain of the patient, the existing algorithm could not calculate the dose perturbation near the surface of the implant. Therefore, Monte Carlo simulations were used to examine the dose enhancement effects in the tissues near the implant by taking into account the physical properties of the implant, beam energies, and beam sizes.

METHODOLOGY

The Monte Carlo system employed in the present work was the PRESTA (Parameter Reduced Electron-Step Transport Algorithm) version of the EGS4 (Electron Gamma Shower) computer code. Detailed descriptions of the structure of the EGS4 code can be found in Ref. 5. In the simulations, the patient's head was modeled by a spherical water phantom 160 mm in diameter. A rectangular coordinate system was assigned to the patient in the simulations. The x axis was along the patient's right to left side. The y axis was along the patient's inferior to superior direction. The z axis was along the patient's posterior to anterior direction. The origin was at the center of the spherical phantom.

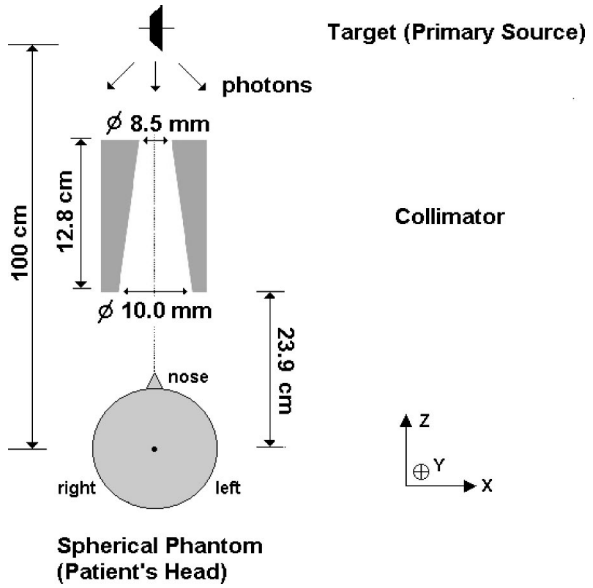

FIG. 1. The EGS4 geometry used in modeling the XKnife® stereotactic radiosurgery system with the 12.5 mm collimator.

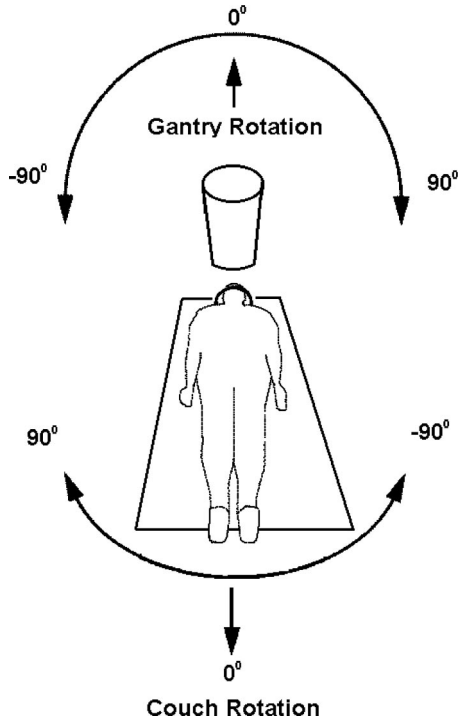

FIG. 2. The angle conventions used by XKnife®.

Because of the large distance (100 cm) between the source target and the radiation isocenter, the source target was modeled by a point. The detailed modeling geometry is shown in Fig. 1. To simplify the simulation geometry, a platinum implant was modeled by a 2-mm-radius sphere at the centre of the water phantom. The 2 mm radius was appropriate for both the order of magnitude of common implants and the resolution of simulation results. The atomic number of platinum is 78 and the density of the pure platinum material is 21.45 g cm^{-3}.

The source target can be moved around the isocenter by different settings of the gantry and couch rotation. Figure 2 shows the angle conventions used by XKnife®. The radiation beam passed through the opening of the collimators to reach the target point. The diameters of the radiation beams at the focus were confined by the collimator system.

In this study, a 12.5-mm-diameter collimator was employed. The collimator confined the circular field size of the beam and for this collimator the field size was a 10 mm diameter at the exit hole of the collimator. Single isocenter with couch rotation 90° and gantry rotations from 30° to 60° were delivered at the center of the spherical water phantom. Scoring bins with dimensions $0.5\times0.5\times0.5$ mm^3 were set up along the three main principal axes. The absorbed dose values were obtained by dividing the energy depositions in the scoring bins by their masses.

A total of 1.5×10^8 histories were obtained in the simulations. The history runs were divided into 10 batches for calculation of statistics. The standard errors for all calculations were 1%. The uncertainties away from the maximum were smaller than 1% because of more generation of secondary particles and thus more energy depositions. The simulation duration for 5000 history runs took on average 25 s in a Windows ME®-based Pentium 4, 1.4 GHz CPU PC with a PowerStation 4.0 Fortran compiler. The input photon spectrums of the 4, 6, and 10 MV are based on Mohan *et al.*[6] The cutoff energies for electrons and photons were set to be 0.521 and 0.01 MeV, respectively. A long-sequence random number generator[7] was employed. This has a sequence length of about 10^{43}, effectively infinite for our calculations, and has about 10^9 independent sequences that can be selected from initial conditions.

RESULTS

Figures 3–5 show the comparisons of the relative doses for the cases with and without the presence of platinum objects for the 6 MV stereotactic radiosurgery system along the *x*, *z*, and *y* axes (ICRU notation), respectively.

Since the radius of the platinum implant was 2.0 mm in size, we focused on the water-platinum interface at the positive and negative values of 2 mm for the *x*, *y*, and *z* axes. The maximum dose received in water was more important than the dose received inside the platinum implant. For example, in Fig. 3, a dose enhancement of $[(135-95)/95]\times100\%=42\%$ is observed close to the platinum object at $x=\pm2$ mm on both positive and negative sides along the *x* axis. The dose enhancement is due to the generation of secondary electrons from photoelectric effect and pair production.

Since there are more photons coming from along the positive *z* axis, a dose enhancement of a maximum of 50% is observed at the positive *z* axis (Fig. 4). There is an underdose close to the platinum object at the negative *z* axis where photons are attenuated just after passing through the plati-

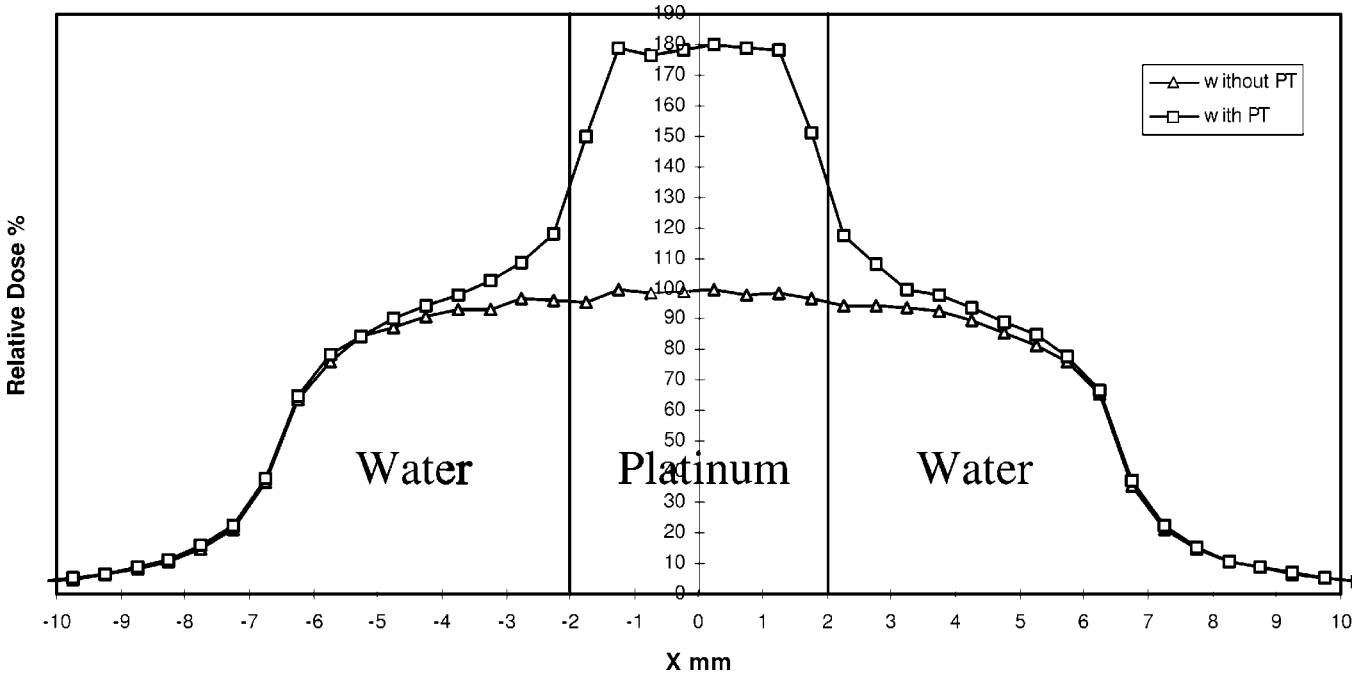

FIG. 3. Comparison of the relative dose along the *x* axis for the cases with and without the presence of platinum objects for the 6 MV stereotactic radiosurgery system with a 12.5-mm-diameter collimator. Dose enhancements were observed close to the platinum implant (i.e., $x=-2$ mm and +2 mm).

num object. The result is similar to the case along the *y* axis in Fig. 5. A maximum dose enhancement of 51% is observed at the positive *y* axis.

In the case of the 4 MV stereotactic radiosurgery system, similar trends are observed when comparing with the case of the 6 MV system. A maximum dose enhancement of 32% is observed at both positive and negative sides of the *x* axis, 46% at the positive side of the *z* axis and 45% at the positive side of the *y* axis. In the case of the high-energy 10 MV stereotactic radiosurgery system, similar trends are also observed when comparing with the case of the 6 MV system, except that the smaller underdose at the negative side of the

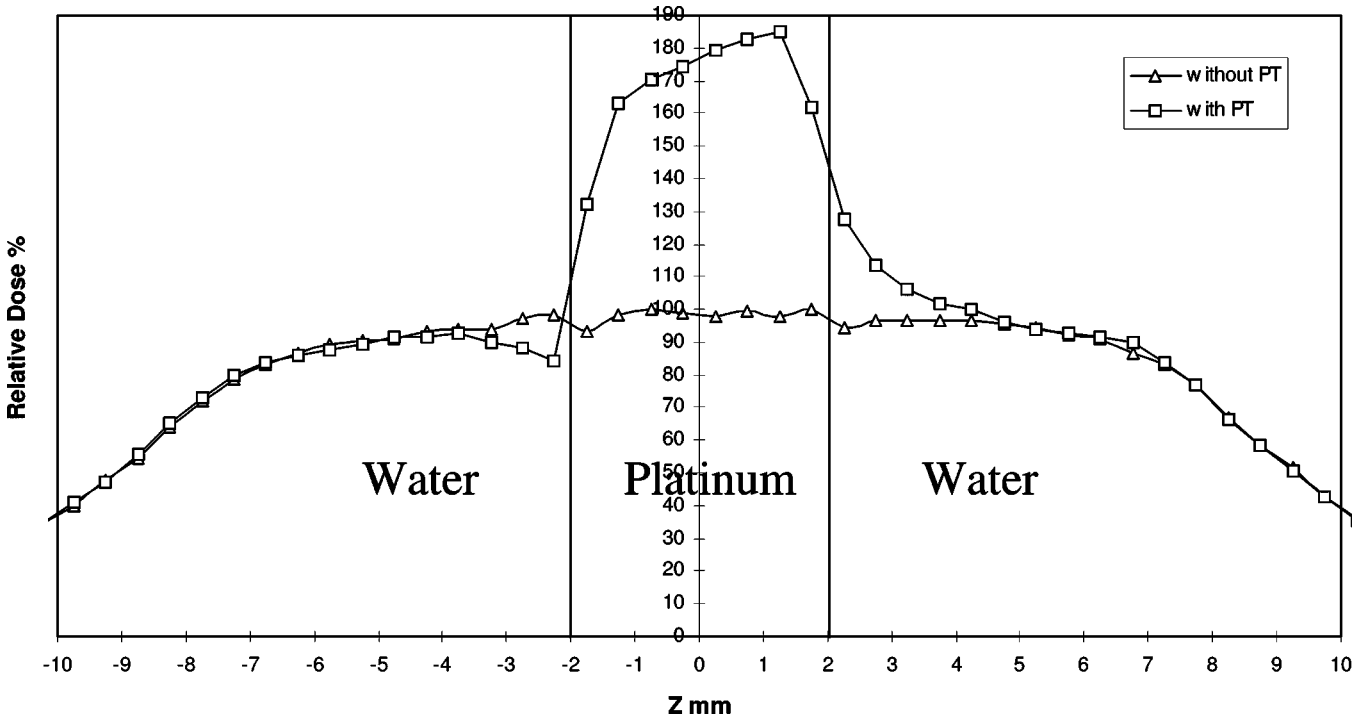

FIG. 4. Comparison of the relative dose along the *z* axis for the cases with and without the presence of platinum objects for the 6 MV stereotactic radiosurgery system with a 12.5-mm-diameter collimator. Dose enhancements were observed close to the platinum implant (i.e., $z=-2$ and +2 mm).

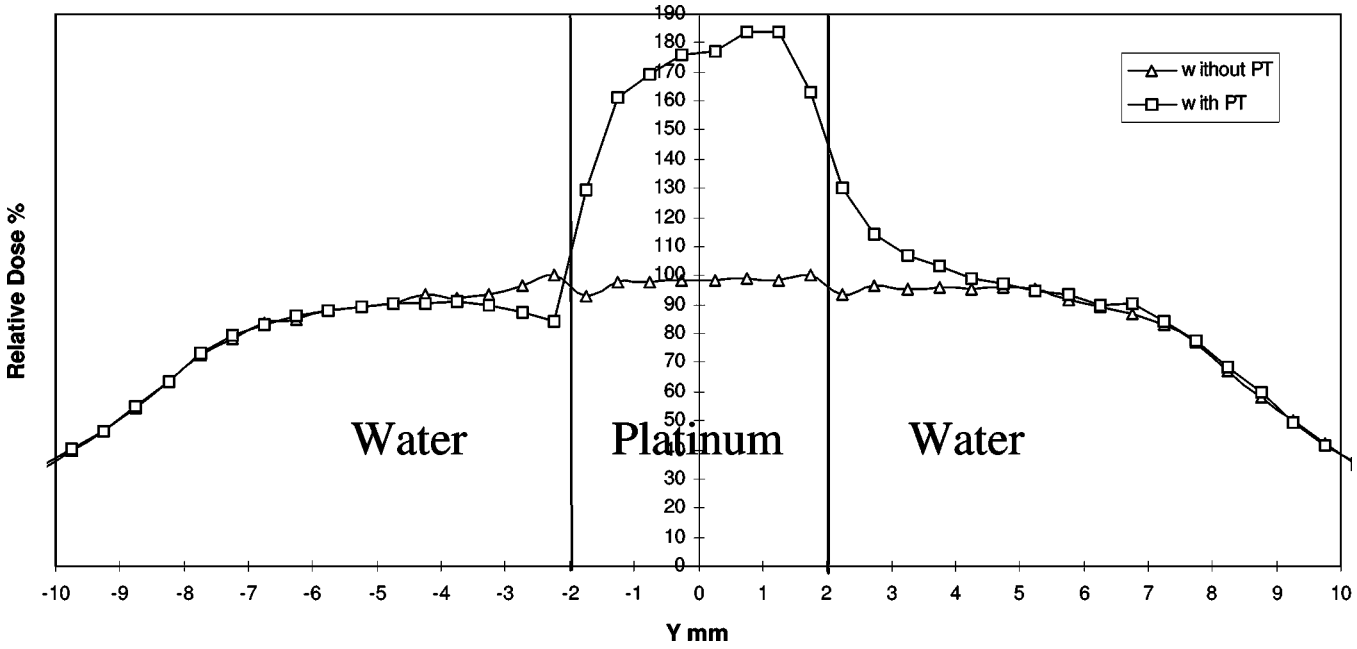

FIG. 5. Comparison of the relative dose along the *y* axis for the cases with and without the presence of platinum objects for the 6 MV stereotactic radiosurgery system with a 12.5-mm-diameter collimator. Dose enhancements were observed close to the platinum implant (i.e., $y=-2$ and +2 mm).

y and *z* axes due to the attenuation become smaller. A maximum dose enhancement of 60% is observed at both positive and negative sides of the *x* axis, 68% at the positive side of the *z* axis, and 67% at the positive side of the *y* axis. Therefore, the dose enhancement increases with the beam energy.

DISCUSSION

All the simulations were repeated using a smaller collimator of 7.5 and 4.0 mm at 6 MV photon energy. The results showed that dose enhancements due to the high-atomic-number platinum implant are significantly higher. For the 7.5 mm collimator, a maximum dose enhancement of 56% was observed at both positive and negative sides of the *x* axis, and 68% at the positive sides of both the *z* and *y* axes. For the 4 mm collimator, a maximum dose enhancement of 160% was observed at both the positive and negative sides of the *x* axis, 56% at the negative sides of both the *z* and *y* axes, and 106% at the positive sides of both the *z* and *y* axes. No underdose regions were found due to domination of high dose enhancements.

Therefore, the dose enhancement was sensitive to both the beam size and the beam energy. The larger collimators resulted in smaller dose enhancements because the increase of scattering partially washed out the dose enhancements. Moreover, a higher beam energy enhanced the pair production process, and therefore more secondary electrons were generated to increase the dose enhancement. Table I shows the relative importance of photon interactions in the simulation with the platinum implant. The proportion of photoelectric effect and pair production increases with the photon energy.

TABLE I. The relative importance of photon interactions in the Monte Carlo simulations with the platinum implant.

	4 MV	6 MV	10 MV
Photoelectric effect	0.05% ± 0.01%	0.10% ± 0.01%	0.20% ± 0.01%
Compton effect	90.2% ± 0.1%	89.5% ± 0.1%	88.1% ± 0.1%
Pair production	9.8% ± 0.1%	10.4% ± 0.1%	11.7% ± 0.1%

The overall dose enhancements observed are higher than those obtained for the Leksell Gamma Knife®.[8] This is due to the large portion of low-energy as well as high-energy photons in the output of the XKnife® stereotactic radiosurgery system. As regards the photon–platinum interaction, photons with energy less than 0.5 MeV favor the occurrence of the photoelectric effect, while photons with energy higher than 4 MeV favor the occurrence of pair production. The Leksell Gamma XKnife® employs ^{60}Co with energies of 1.173 and 1.333 MeV as radiation sources. Therefore, the cross sections for the photoelectric effect and pair production are higher for the XKnife® than the Leksell Gamma XKnife® stereotactic radiosurgery system when irradiating platinum materials.

The XKnife® radiosurgery TPS can only reproduce the Monte Carlo results at radial distances far away from the platinum implant, since the algorithm of the XKnife® TPS presumes a homogeneous water equivalent phantom only. The Monte Carlo results for the dose distribution close to the platinum implant in XKnife® stereotactic radiosurgery are difficult to be obtained through physical measurements. Radiochromic films have a high spatial resolution and are therefore suitable for obtaining dose profiles from collimator outputs.[9] However, the spatial resolution given by the films is basically limited by the densitometer. The mechanical

movement of the sensor during the scanning of the film and the energy dependency[10] of radiographic films introduce experimental uncertainties.

CONCLUSIONS

Dose enhancements have been observed in XKnife® stereotactic radiosurgery systems when platinum implants, such as GDC or ABI, are within the target region. Particular care should be taken in the XKnife® stereotactic radiosurgery when irradiating platinum objects that are close to some vital brain structures. The dose enhancement is sensitive to both the beam size and the beam energy. In particular, the dose enhancement increases with beam energy but decreases as beam size increases. The calculated enhanced doses due to secondary electrons exiting from the high-atomic-number platinum implant can serve as a reference for XKnife® stereotactic radiosurgery centers throughout the world.

ACKNOWLEDGMENTS

We acknowledge useful discussions with and professional suggestions by Dr. P. M. Wu, senior physicist at the Queen Mary Hospital of Hong Kong.

[a]Author to whom correspondence should be addressed; electronic mail: peter.yu@cityu.edu.hk

[1]T. W. Malisch, G. Guglielmi, F. Vineula, G. Duckwiler, Y. P. Gobin, N. A. Martin, and J. G. Frazee, "Intracranial aneurysms treated with the Guglielmi detachable coil: midterm clinical results in a consecutive series of 100 patients," J. Neurosurg. **87**, 176–183 (1997).

[2]D.E. Brackmann, W. E. Hitselberger, R. A. Nelson, J. Moore, M. D. Waring, F. Portillo, R. V. Shannon, and F. F. Telischi, "Auditory brainstem implant: I. Issues in surgical implantation," Otolaryngol.-Head Neck Surg. **108**, 624–633 (1993).

[3]R. D. Evans, *The Atomic Nucleus* (McGraw-Hill, New York, 1955).

[4]XKnife 4.0. Radionics Software Applications Inc., Burlington, Massachusetts (1998).

[5]W. R. Nelson, H. Hirayama, and D. W. O. Rogers, The EGS4 Code System SLAC-265, Stanford Linear Accelerator Center, Stanford University, Stanford, California 94305 (1985); http://www.slac.stanford.edu/egs/

[6]R. Mohan, C. Chui, and L. Lidofsky, "Energy and angular distributions of photons from medical linear accelerators," Med. Phys. **12**, 592–597 (1985).

[7]F. James, Report DD/88/22, CERN-Date Handling Division, 1988.

[8]J. Y. C. Cheung, K. N. Yu, J. F. K. Chan, R. T. K. Ho, and C. P. Yu, "Dose distribution close to metal implants in Gamma Knife Radiosurgery: A Monte Carlo study," Med. Phys. **30**, 1812–1815 (2003).

[9]M. J. Butson, K. N. Yu, T. Cheung, and P. E. Metcalfe, "Radiochromic film for medical radiation dosimetry," Mater. Sci. Eng., R. **41**, 61–120 (2003).

[10]A. S. Meigooni, M. F. Sanders, G. S. Ibbott, and S. R. Szeglin, "Dosimetric characteristics of an improved radiochromic film," Med. Phys. **23**, 1883–1888 (1996).